METABOLIC CHARACTERIZATION OF HUMAN OVARIAN CARCINOMA BY ^{1}H-NMR SPECTROSCOPY

A. Ricci[1*], E. Iorio[1], M. Pisanu[1], R. Canese[1], S. Canevari[2] and F. Podo[1]
[1]Department of Cell Biology and Neurosciences, Section of Molecular and Cellular Imaging, Istituto Superiore di Sanità, Roma; [2]Department of Experimental Oncology and Laboratories, Unit of Molecular Therapies, IRCCS Fondazione Istituto Nazionale Tumori, Milano.

**** Biophysics PhD course(XXII cycle), School of Biology and Molecular Medicine***

ABSTRACT

There is today an increasing interest in studies reporting high levels of choline containing compounds (tCho), notably phosphocholine (PCho) in cancers in vivo and in vitro as compared to the corresponding non tumoral cells and tissues. Only a few studies have focused attention on ovarian cancer, a neoplasia portrayed as an insidious disease or silent killer that causes no symptoms and is hardly detected at first stages, with a 5-year survival still remaining at about 44%. Purpose of the present study is to evaluate the biochemical and functional significance of aberrant tCho content in ovarian cancer. To this end, we used different preclinical models and surgical samples analyzed by a number of magnetic resonance spectroscopy (MRS) techniques, i.e. in vitro ^{1}H MRS of cells and tissue extracts, in vivo MRS of EOC xenografts in immuno-deficient mice, ex vivo High Resolution (HR) MRS and magic angle spinning (MAS) analyses of intact tissues samples, complemented with the molecular biological approaches.

Key works: Ovarian Cancer, Phosphatidylcholine metabolism, Phosphocholine, high resolution magic angle spinning.

METABOLIC CHARACTERIZATION OF HUMAN OVARIAN CARCINOMA BY ^{1}H NMR SPECTROSCOPY

INTRODUCTION

Magnetic resonance spectroscopy (MRS) has been extensively used for over thirty years to investigate biochemical pathways in organs and tissues in living systems. Today there is a general agreement on the value of MRS in diagnosis, prognosis and therapy monitoring in a number of pathologies. In particular, MRS offers powerful approaches to detect metabolic alterations associated with cell malignant phenotypes and investigate the underlying molecular mechanisms **[1,2,3,4]**.

Several studies, in fact, have shown higher levels of choline-containing metabolites (tCho) and in particular phosphocholine (PCho) in different types of cancer in vivo and in vitro, compared with the corresponding non-tumoral tissues and cells **[5,6,7]**.

Only a few studies have focused attention on ovarian cancer. This neoplasia is portrayed as an insidious disease or silent killer that causes no symptoms and is hardly detected before widespread metastasis formation in the abdominal cavity, with frequent recurrences, and a 5-year survival still remaining at about 44% **[8]**. The existing gaps in the knowledge of the molecular mechanisms responsible for EOC progression lead to the current limitations of therapy regimens, mainly restricted to the use of cytotoxic drugs and often associated with side effects and onset of drug resistance.

Our research group focused, as first, attention on alterations of the tCho spectral profile in EOC cell lines in relation to tumor progression from normal ovary epithelial cells (OSE) to non-tumoral immortalized cell variants (IOSE, hTERT), to EOC cell lines **[9]**. The tCho pool was found to increase 2.0- to 3.5-fold in EOC cells compared with the whole set of non tumoral (EONT) cells, with parallel 3- to 8-fold increase in PCho, the most abundant Cho derivative, whose signal accounted for 75% ± 6% of the overall tCho resonance. Elucidation of the mechanisms responsible for aberrant PC metabolism may allow identification of novel biomarkers of tumour progression and development of new targeted anticancer therapies.

Since the observed changes in PCho in both breast and ovary cancer cells did not directly correlate with altered cell doubling time, it was suggested that intracellular PCho accumulation in cancer cells does not simply reflect increased cell tumor proliferation, but is more likely linked to gene-driven alterations of PC-cycle enzymes, as a consequence of the aberrant activation of multiple cell signaling pathways **(Fig. 1)**.

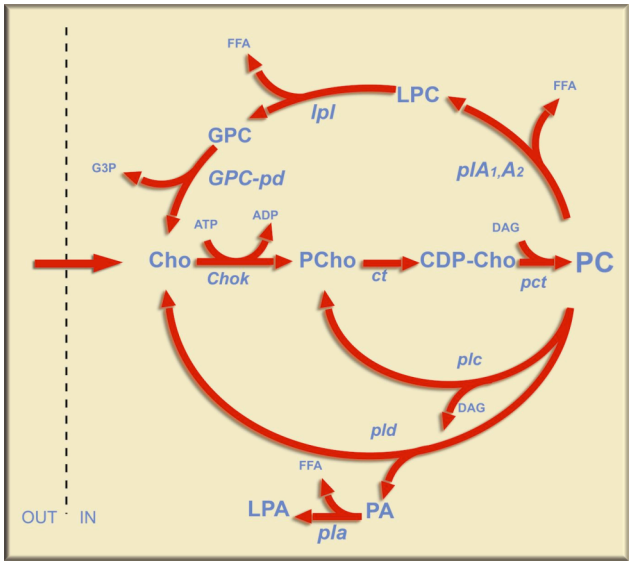

Figure 1. Schematic representation of phosphatidylcholine (PC) de novo biosynthesis and catabolism.
Metabolites: CDP-Cho, CDP choline; Cho, choline; DAG, diacylglycerol; FFA, free fatty acid; G3P, sn-glycerol-3-phosphate; GPC, glycerophosphocholine; LPA, lysophosphatidate; PA, phosphatidate; PCho, phosphocholine.
Enzymes: ChoK, choline kinase; ct, cytidylyltransferase; lpl, lysophospholipase; pct, phosphocholine transferase; GPC-pd, glycerophosphocholine phosphodiesterase; plA_1, phospholipase A_1; plA_2, phospholipase A_2; plc, phospholipase C; pld, phospholipase D.

Purpose of the present work was aimed at: 1) elucidating the molecular mechanisms responsible of aberrant PC metabolism in cultured EOC cells; 2) investigating the significance of the tCho profile in preclinical and clinical EOC biopsies, as indicators of cancer prognosis and follow up in intact tissues and their extracts.

Materials and Methods

Preclinical Models

For detailed description of all topics in this section see the Appendix.

High resolution NMR spectroscopy of cells and tissues extracts.

High-resolution NMR experiments (25°C) were performed at either 400 or 700 MHz (Bruker AVANCE spectrometers, Karlsruhe, Germany). ^{1}H MRS spectra of cell and tissues extracts were obtained using acquisition pulses, water pre-

saturation, data processing and data analysis as already described **[9]**. Quantification of individual metabolites was obtained from peak areas using correction factors determined by experiments at the equilibrium of magnetization (90° pulses, 30.00 s interpulse delay). Metabolite quantification was expressed as nmoles and normalized to the number of extracted cells.

In vivo MRI/MRS of tumor xenografts

Experiments were performed on a Varian INOVA MRI/MRS system operating at 4.7 T, equipped with actively shielded gradient coils (maximum gradient strength 120 mT/m; rise time <150 μs), with a transmitter volume RF coil actively decoupled from the receiver surface coil (RAPID Biomedical, Rimpar, Germany), in order to get over the RF homogeneity issue and exploit the S/N benefit of surface coil technology. Anaesthesia was induced with isofluran 2.5% in O_2, 1 liter/min, directly administrated to the animal already positioned in the slide.

High resolution NMR spectroscopy of intact tissues

High Resolution Magic Angle Spinning (HRMAS) were performed on intact preclinical and clinical tissues. The tissue samples were put in cryogenic vials and immersed in liquid nitrogen immediately after dissection. Samples were stored for 2-5 months before HRMAS analysis. All tissue samples were cut to fit a 4 mm zirconia rotor with insert (total sample volume 12 μL). Before insertion into the rotor, the sample was immersed in physiological solution (NaCl 0.9% in D_2O) containing TSP as a internal standard for chemical shift reference. Excess fluid was removed at the end of the rotor assembling procedure. The weight of added buffer and wet-weight of the sample were accounted for by repeated weighing of the rotor during the assembly procedure. HRMAS experiments were performed on a Bruker AVANCE 400 MHz spectrometer equipped with a ^{1}H MR probe with a gradient aligned with the magic angle axis (Bruker BioSpin, Karlsruhe, Germany). Samples were spun at 3 kHz and all experiments were performed at an instrumental temperature setting of 4°C. Seven sets of one-dimensional experiments were performed for each sample. A single pulse experiment with 3.0 sec of pre-saturation was performed using pulse angle of 90° over a sweep width of 12 ppm. The FID was acquired into 32 K points during an acquisition time of 3.41 s, resulting in a repetition time of 6.41 s; 128 transients were collected. Carr Purcell Meiboom Gill (CPMG) experiments were performed using 2.5 sec of water suppression prior to a 90° excitation pulse. A total of 128 transients were collected over a sweep width of 12 ppm into 32 K points, giving an acquisition time of 3.41 sec. T2 filtering was obtained using a delay of 1 msec repeated 0, 32, 64, 160, 320, 360 times respectively resulting, in a 0, 64, 128, 320, 640 and 720 msec effective echo time. All HRMAS experiments were performed within 87 min from tissue defrosting. Spectral assignments were performed based on literature data and comparative analyses were carried out on spectra obtained from tissue extracts.

Statistical analysis.

Data were analyzed using GraphPad software version 3.03. Statistical significance of differences was determined by one-way ANOVA or by Student t-test (as specified). Differences were considered significant at $p < 0.05$.

Results and Discussion

1. Activation in EOC of enzymes responsible for PCho production

1 a. Intracellular levels of choline containing metabolites in EONT and EOC cells

In agreement with previous analyses **[9,11],** quantitative high-resolution ^{1}H-MRS analyses at high field allowed us to measure a tCho content of 5.4 ± 0.6 nmol/10^6 cells (corresponding to a cellular average concentration of about 2.0 mM) in aqueous extracts of normal ovary surface epithelial cells and their immortalized non-tumoral cell variants (EONT). With respect to this basal level, the tCho content measured in different EOC cell lines (SKOV3, CABA I, IGROV1, OVCAR3) reached much higher intracellular levels (4.0 to 7.0 mM). The most remarkable feature was a 3.0- to 8.0-fold increase in PCho in EOC with respect to EONT cells (**Fig. 2).** The average percent contribution of this metabolite to the overall tCho resonance profile increased from about 50% in EONT to 70-90% in EOC cells.

The observed changes in PCho contents in ovary cancer cells with respect to their normal or non-tumoral immortalized counterparts, did not correlate with differences in cell doubling time. This finding represents an important issue in the elucidation of molecular mechanisms associated with altered choline metabolism in cancer. Against previous assumptions, the present body of evidence supports the general hypothesis that an increased PCho concentration is not a simple indicator of the incremented phospholipid production necessary to cancer cells to cope with higher proliferation requirements, but more likely represents the result of the activation of PC-cycle enzymes, under genetically induced changes in growth factor-mediated cell signaling pathways.

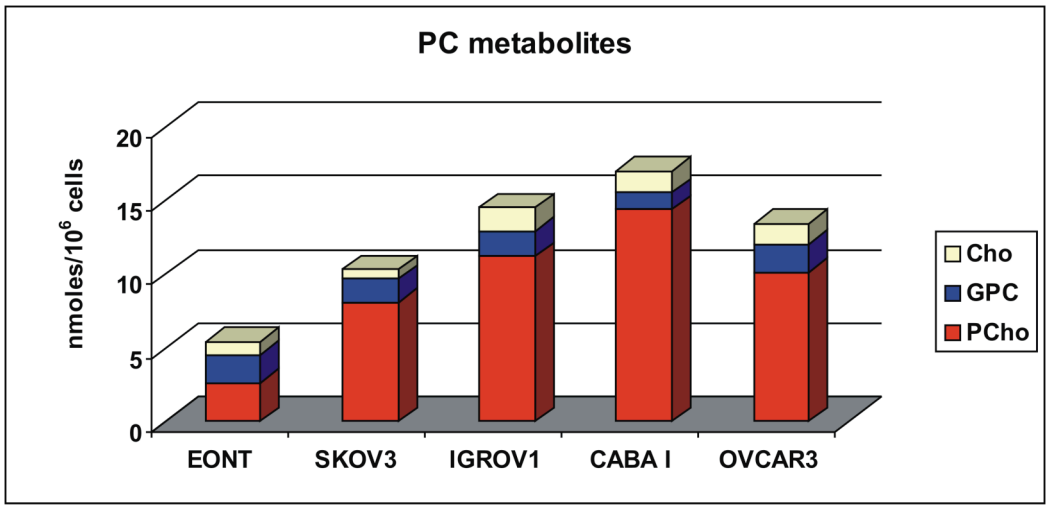

Figure 2. Intracellular concentrations of choline (Cho), phosphocholine (PCho) and glycerophosphocholine (GPC) measured by ^{1}H MRS analysis of aqueous extracts of ovarian normal and immortalized cells (EONT) and carcinoma cells lines (SKOV3, IGROV 1, CABA I, OVCAR3).

1 b. Activation of phosphatidylcholine-cycle enzymes

The observed increases in the intracellular PCho content in ovarian cancer cells may in principle result from activation of different biosynthetic and/or catabolic PC-cycle pathways as outlined in **Fig. 1**.

The *de novo* biosynthesis of PC occurs *via* the three-step Kennedy pathway (also known as the cytidyldiphospho-choline (CDP-Cho) pathway) in which choline is phosphorylated into PCho by choline kinase (Chok), PCho is converted into CDP-choline by cytidylyltransferase (ct) and CDP-choline is incorporated into PC by choline phosphotranferase (pct). While ct mediates the rate-limiting step of the pathway, Chok acts as a regulatory enzyme for PC biosynthesis.

The Chok activity measured in our laboratory in EONT cells was only 0.6 ± 0.1 nmol/10^6 cells·h but increased 12- to 24-fold ($p< 0.001$) in EOC cells [**9,11**].

The increases in Chok activity and PCho levels in EOC cells are in agreement with a substantial body of evidence reported in the literature on implications of this enzyme and its choline-containing product in human carcinogenesis. In this context, the different rates of Chok activity measured in EOC and EONT cells warrant further investigations to elucidate to which extent activation of individual isoforms of this enzyme may act as possible pharmacodynamic endpoints of new

cancer therapies, either based upon specific Chok inhibition or upon selective targeting against cell signaling pathways involved in Chok regulation.

Gene expression analysis, performed at IRCCS Fondazione Istituto Nazionale Tumori Milano (Dr. Canevari and co-workers), showed a significant up-modulation of Chokα in EOC cells (p=0.003) as compared to OSE cells **(Fig. 3)**, associated with a practically all unaltered Chokβ, ct expression and pct expression These results suggest that the overall changes in *ct* and *pct* genes expression could hardly contribute to further accumulation of PCho besides that provided by choline kinase and point to an increase in Chokα-mediated Cho phosphorylation as a major mechanism responsible for the build-up of the PCho pool in the Kennedy pathway in EOC cells **[10; Iorio et al, manuscript in submission]**.

Since we did not find any statistically significant correlation between ChoK activity and PCho levels we also investigated the PC-catabolic pathways. Three major catabolic pathways can contribute to the rate of formation of MRS-detected intracellular PCho pools: phospholipase C-mediated (PC-plc) PC hydrolysis into PCho and diacylglycerol; combined action of PC degradation by phospholipase D (pld) into Cho and phosphatidate and further phosphorylation by Chok of Cho into PCho; phosphodiesterase (pd)-mediated hydrolysis of GPC into Cho and glycerophosphate and subsequent Cho phosphorylation . The last reaction represents the terminal step of PC degradation along the deacylation pathway mediated by the combined action of phospholipases A2 and A1 (pla) and lysophospholipases (lpl).

Assays on PC catabolism carried out in our laboratory by measuring Cho formation in total cell lysates of EONT and EOC cells following addition of monomeric, short-chain PC (1,2-dihexanoyl-*sn*-glycero-3-phosphocholine, C6PC) showed that PC-plc activity increased 4- to 17-fold in EOC cells, while pld and GPC-pd were only activated about 2- to 3-fold in some, but not in all EOC cells. Regarding the deacylation pathways we found a lower activity of PLA2 in EOC compared with EONT cells. The overall body of results overviewed in this section shows that both biosynthetic and catabolic PC-cycle pathways may contribute to the increased MRS-detected PCho levels in cancer cells **(Fig. 4)**.

MRS analyses confirmed a PC-plc role in modulating the intracellular PCho content. In fact, when OVCAR3 cells were exposed to the PC-plc inhibitor tricyclodecan-9-yl-potassium xanthate (D609, 200 μM), we observed a significant drop (by about 50%;) in the PCho content, detected within 24h of treatment. These effects were associated with a reduced cell growth **(Fig. 5) [10]**.

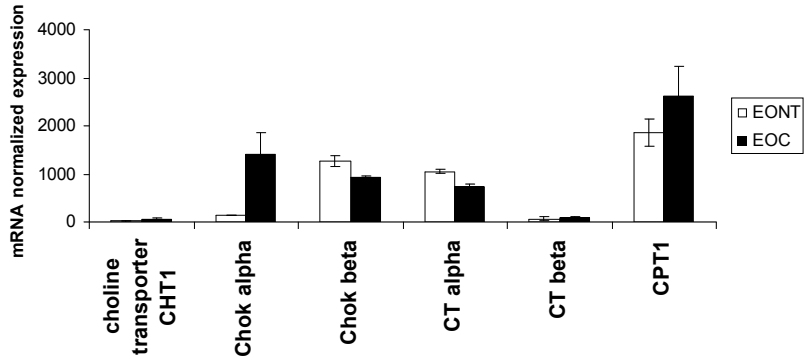

Figure 3. Normalized mRNA expression of genes involved in Kennedy pathway. CHT1, choline trasporter 1; ChoK alpha, choline kinase α; ChoK beta, choline kinase β; CT alpha, cytidylyltransferase α; CT beta, cytidylyltransferase β; CPT1, phosphocholine tranferase.

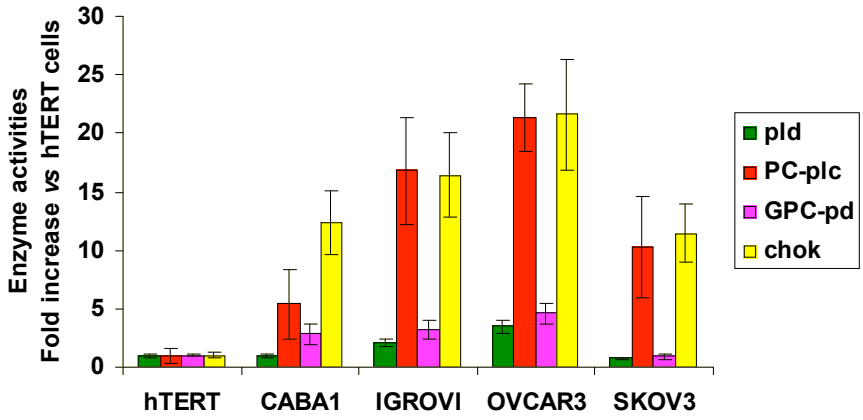

Figure 4. Increases in activity rates of PC cycle enzymes in EOC compared with EONT cells: pld , phospholipase D; PC-plc, phospholipase C; GPC-pd, glycerophosphocholine-phosphodiesterase; choK, choline kinase.

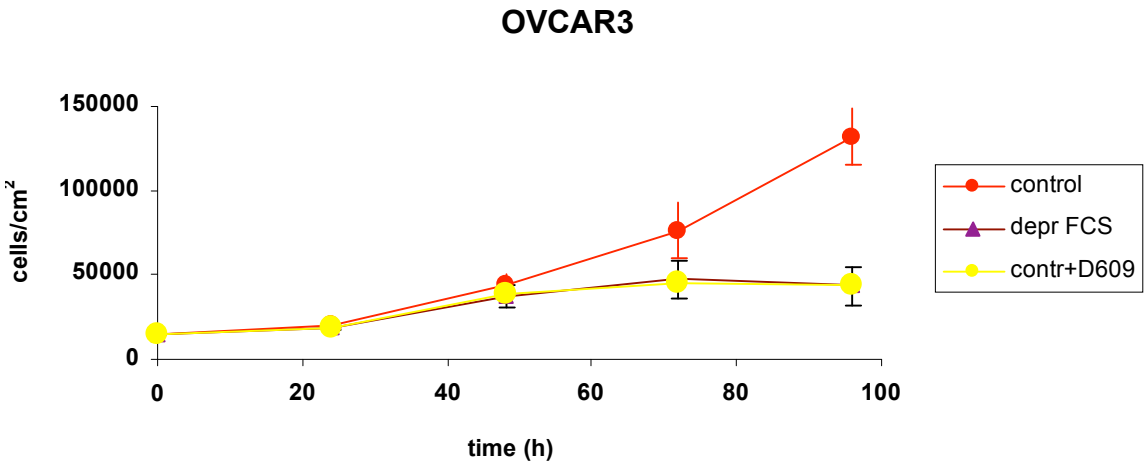

Figure 5. Anti-Proliferative effect of PC-plc inhibitor (D609) and serum deprivation on OVCAR3 cells

The overall results of in vitro assays showed that two enzymes are strongly activated in EOC compared with EONT cells, ChoK and PC-plc.

A number of studies have shown overexpression/activation of ChoK in cancer tissues and cells **[7,13,14]**.

Furthermore, down-modulation of ChoK resulted in a drop of intracellular PCho level associated with a reduced cell growth in cancer cells in vivo and in vitro **[15,16]**.

Regarding PC-plc, we showed for the first time, that this enzyme was responsible at least for 30% of the PCho signal. Moreover, our group reported evidence on the role of PC-plc in cell proliferation of growth-factor stimulated or tumour cells **[17,18]**. Thus, both ChoK and PC-plc enzymes could participate on signalling in EOC, and their inhibition may represent new means of designing targeted anti-cancer treatments.

In this context, preliminary results in our laboratory showed a linkage between cell signalling cascades triggered by receptor-ligand interaction and the activity of PC-plc. In fact, inhibition of PC-plc activity with D609 induced a strong down-modulation of CXCR4, a receptor involved in the metastatic process of malignant tumours **[19]**.

2. Characterization of the ^{1}H MRS choline signal in preclinical models

2 a. In vivo MRS of EOC xenografts in SCID mice

In order to develop a suitable method to test and monitor by MRS biochemical effects of either conventional or new targeted therapies we established an in vivo

model of human EOC transplanted in immunodeficient mice. In particular, we first developed an SKOV3 cell variant (SKOV3 ip) obtained by in vivo passage of SKOV3 cells (over-expressing HER2) in the peritoneum of Severe Combined Immunodeficiency (SCID) mice. This cell variant, which was associated with enhanced in vivo tumorigenicity, as detected by faster in vivo growth and reduced survival of the tumour bearing-mice, exhibited an about two fold higher PCho content **(Fig. 6)**. Preliminary experiments in our laboratory also showed a 2-fold higher ChoK activity in these cells.

Two models were obtained by either orthotopic, intraperitoneal (IP), or heterotopic, subcutaneous (SC) implantation of SKOV3 ip in SCID mice.

In vivo quantification of the tCho signal in both types of xenografts **(Fig. 7)** gave an average concentration of 6.0 mM, in agreement with analysis on cells extracts **[20].**

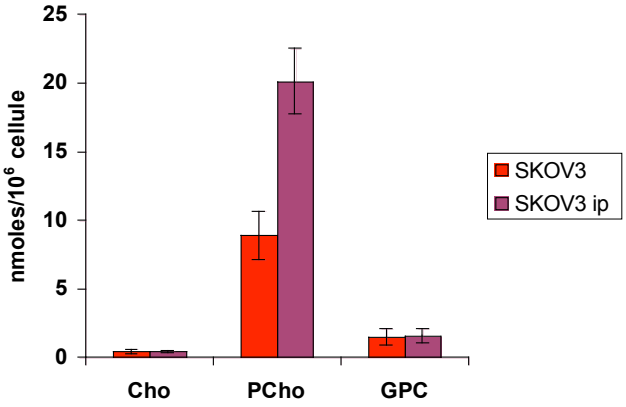

Figure 6. Choline containing metabolites
(Cho, PCho, GPC) of parental cell line SKOV3 and its intraperitoneum in vivo passaged variant SKOV3 ip.

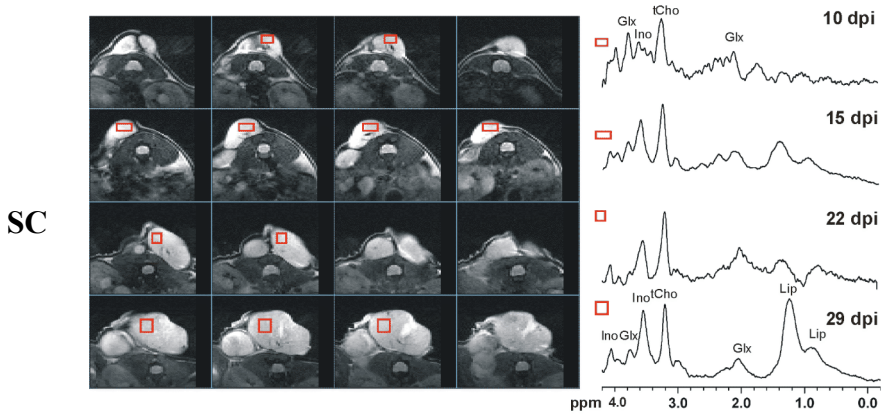

Figure 7. Examples of MRI/MRS of subcutaneous (SC) tumor derived from the injection of 5 x10^6 SKOV3 cells during growth. (MRI : TR/TE = 2000/70 ms, 2 transients, 19 slices, FOV = 30 x 30 mm^2, matrix 256 x 128, thickness = 1 mm which corresponds to pixel resolution of 117 x 234 x 1000 μm; MRS spectra were acquired from the voxels indicated in the respective images, by using a PRESS sequence (TR/TE = 2000/23 ms, 256 transients, VOI ranging from 3 to 12 μl). **Metabolites:** Lip, lipid; Glx, glutamine + glutamate; tCho, choline containing compounds; Ino, myo-inositol.

2 b. Monitoring the effects of in vivo cisplatin therapy on ex vivo ^{1}H MRS spectra

Since several studies indicated alterations in ^{1}H MRS spectral profiles of tumours following anticancer treatments **[1,2,3]**, we investigated the effects on MR spectra signals of tissues isolated from EOC xenografts after treatment with cisplatin (cis), a conventional EOC chemotherapeutic agent.

Tissue samples were analyzed at the end of the third treatment (about 21 days after the first administration). At this time, the weight of cisplatin-treated was remarkably lower that of control tumour **(Fig. 8)**.

Under these conditions, the tumour proliferative index (measured by Ki67) decreased from 40% to 15%. With no induction of necrosis, determined by histopathological analysis **(Fig. 9)**.

Simultaneously, the PCho content in aqueous tissues extracts significantly decreased about 23% (p=0.02; n=10) in cisplatin-treated compared with untreated tumours **(Fig. 10)**, suggesting that this metabolite may be considered as a possible endpoint of EOC therapy response, while the other metabolites did not undergo any statistically significantly changes.

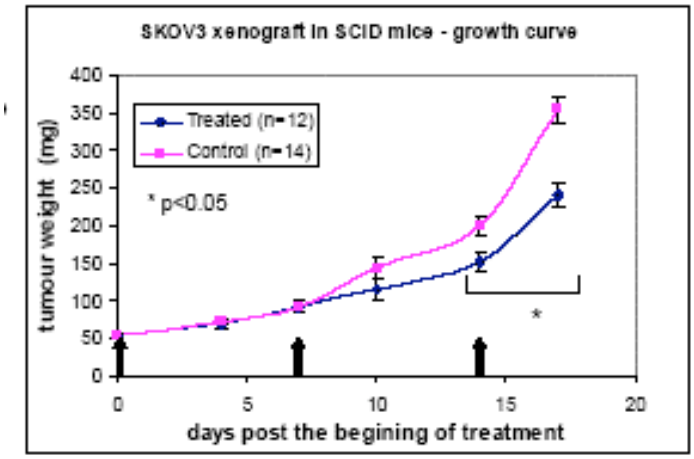

Figure 8. Tumor weight in untreated and treated mice ($p<0.05$).
Black arrows indicate the days of treatments. Dose of administrated cisplatin: 5 mg/Kg.

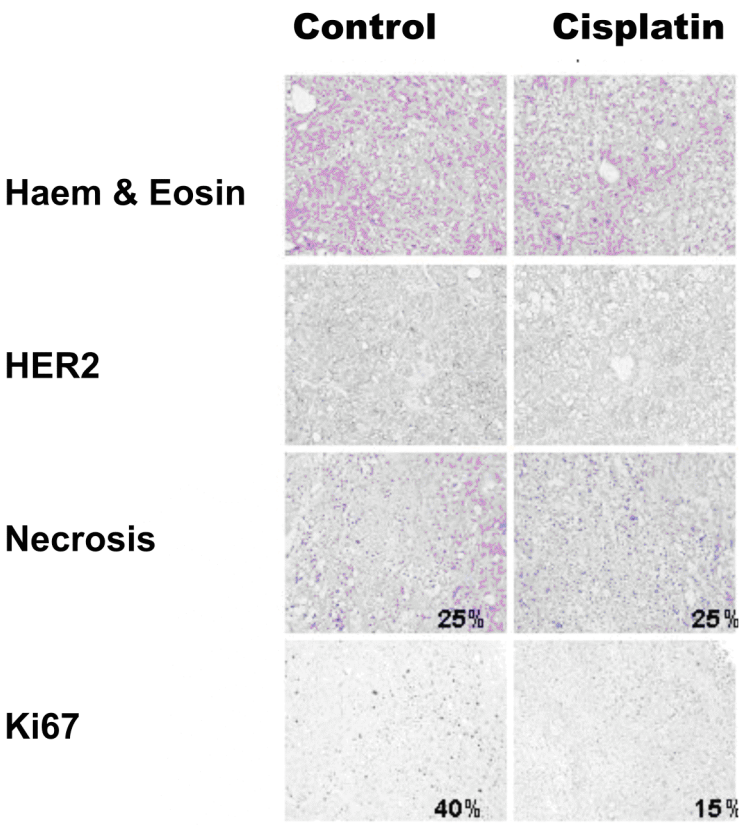

Figure 9. Histophatologic and himmunohysto-chemistry analysis of untreated and cisplatin treated xenografts. From the above:
1) Hematoxylin-eosine
2)HER2 expressions: marker of aggressiveness.
3)Necrosis percentage
4)Ki67: proliferative index

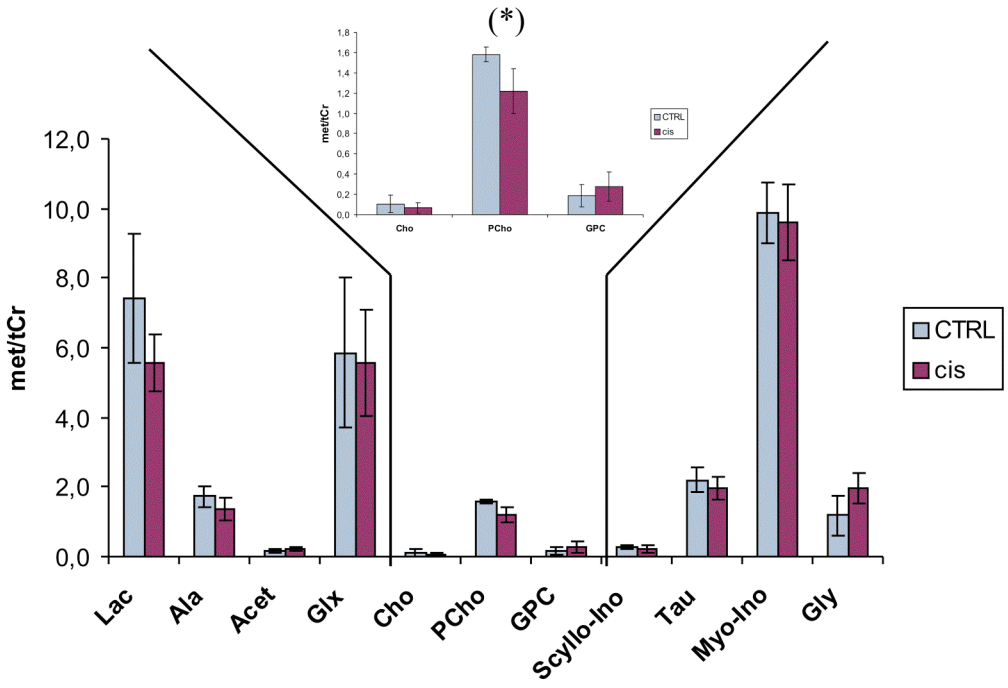

Fig 10. Effect of cisplatin (cis) treatment on the relative levels of ^{1}H MRS detected metabolites in subcutaneous SKOV3 ip xenografts. (n=4 for each group).
(*) PCho, p=0.02.

The overall results obtained from analysis of preclinical EOC models (cells and xenografts) indicates that the PCho signal may act as potential indicator for monitoring disease progression and response to therapy.

2 c. High Resolution ^{1}H MRS on intact EOC tissue samples

In order to provide the molecular bases to the interpretation of the spectral tCho profile of clinical EOC lesions, ^{1}H MRS analyses were performed on intact tumour tissues excised from either SC or IP xenografts. To this end, we used the high resolution magic angle spinning (HRMAS) ^{1}H MRS technique, which allows detection of altered metabolite levels in intact tumor specimens, providing a bridge between in vivo MRS and histopathological examinations **[21]**. A major interest is today focused on correlations between the levels of individual choline metabolites under the total choline tCho profile and the percentage of cancer cells in the specimen, as well as tumour aggressiveness and response to therapy **[22]**.

The following metabolites were detected in HRMAS ^{1}H MRS spectra of EOC xenografts: lactate (Lac 1.33 ppm), alanine (Ala, 1.45), total Creatine (tCr, 3.04 ppm), Cho (3.21 ppm), PCho+GPC (3.23 ppm), scyllo-inositol (scyllo-Ins, 3.33 ppm), taurine (Tau, 3.45 ppm) and myo-inositol (myo-Ins, 3.55 ppm). Relative

quantification was performed by normalizing the integral of each metabolite resonances with respect to the integral of tCr (creatine *plus* phosphocreatine) proposed by some investigators **[20]** as suitable internal reference. We did not observe any significant difference in the MRS profile of specimens isolated from the two EOC models **(Fig. 11)**. These analyses confirmed the relative metabolite quantification obtained from in vivo tumours.

Furthermore, we found that PCho was the most intense resonance in the tCho region, suggesting that relative contributions of individual tCho components were not significantly altered by the different in vivo and in vitro experimental growth conditions adopted in our study.

Moreover, the consistency of ^{1}H MRS analyses of the PCho signal in both in vivo and in vitro EOC cells, represented the basis for a better interpretation of the biochemical nature of the tCho resonance at the clinical level.

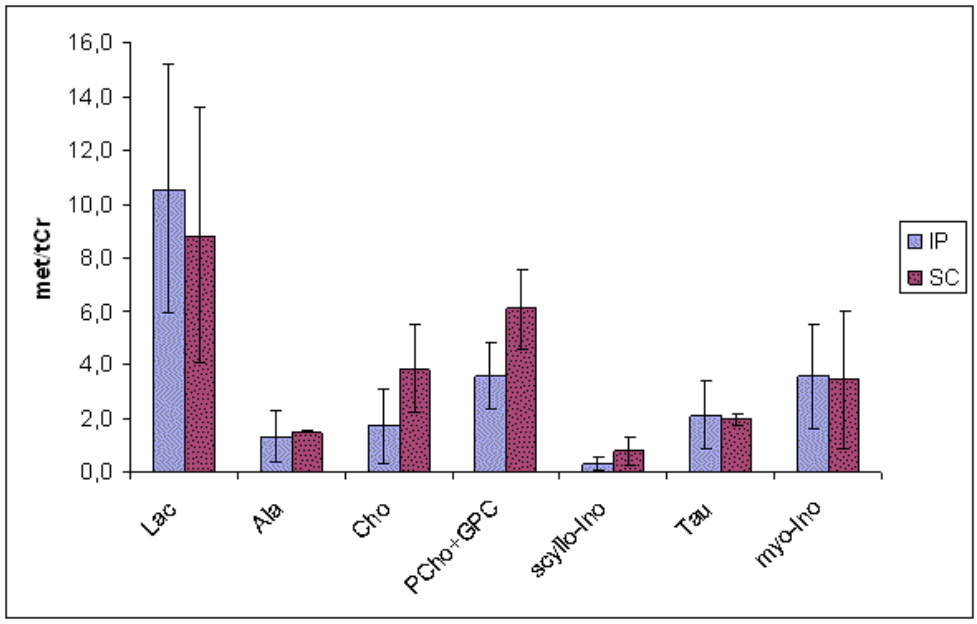

Fig. 11. Differences between ^{1}H HRMAS signals between SC (n=5) and IP (n=5) EOC xenografts in SCID mice (means value ± standard deviation).
Metabolites: Lac, lactate; Ala, alanine; Cho, choline; PCho+GPC: phosphocholine+glycerophosphocholine; Scyllo-Ino, scyllo-inositol; Tau, taurine; myo-Ino, myo-inositol.

3. Characterization of the ^{1}H MRS choline signals in clinical samples

A subset of EOC samples (n=6), isolated from patients with different clinical history (e.g. with differences response to therapy and or in time to relapse), was analyzed by HRMAS ^{1}H MRS and MRS of tissue extracts **(Tab. 1)**. We found in these spectra high levels of free Cho **(**example in **Fig. 12)** comparable or even higher to that PCho. Relatively high Cho contents in the tCho region were also reported on prostate and brain cancer tissues **[23,24]**. With the aim to evaluate if the high level of Cho is an artifact product of surgical EOC sample handling, we set up an experiment on epithelial cancer tissues collected at primary surgery and frozen at different times after dissection. To this purpose, a series of breast cancer tissues, handled under well controlled conditions, was provided by the Istituto Nazionale Tumori (INT, Milano). HRMAS spectra were acquired on four breast carcinoma specimens, whose multiple samples were respectively frozen within 10-40 min, at 2h, 6h, and 24h after dissection). All spectra were recorded at 4°C within 1h on samples of 11.5 ± 2.9 mg (example in **Fig. 13**). Metabolite quantification was performed by HRMAS ^{1}H MRS spectroscopy **(Fig. 14)**.

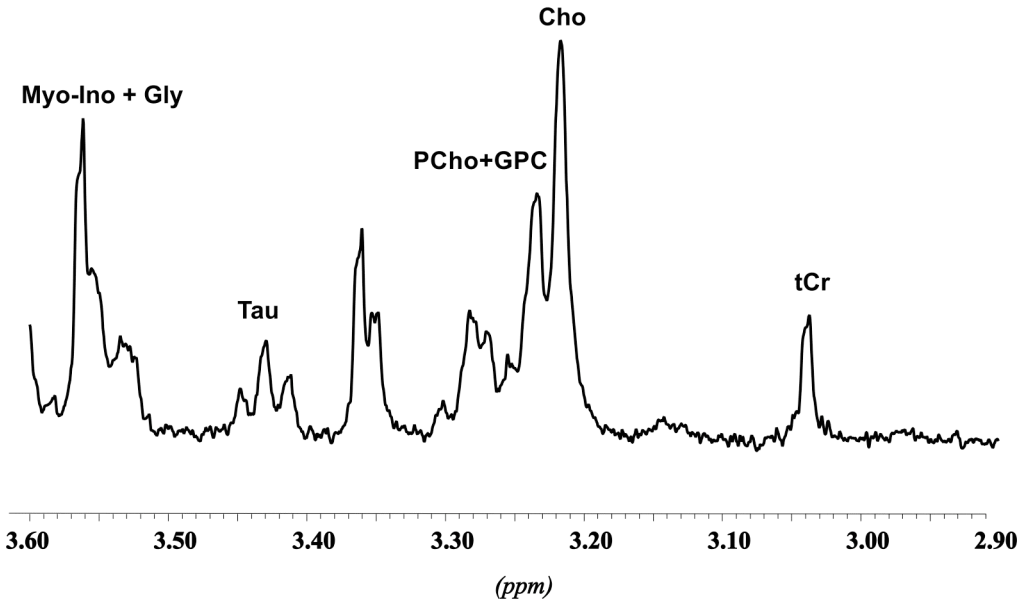

Figure 12. ^{1}H HRMAS spectrum of a surgical specimen isolated from EOC patient.

Tab 1. Relative quantification (met/tCr) of ^{1}H MRS signals in aqueous extracts of surgical samples isolated from two different groups of EOC treated with cisplatin + taxol.

	Time to relapse > 1 year (n=2)	Time to relapse within 1 year (n=4)
Valine	0.84 ± 0.01	0.86 ± 0.12
Lactate	19.34 ± 6.70	12.40 ± 3.36
Alanine	1.90 ± 0.06	2.69 ± 1.49
Acetate	1.79 ± 0.40	0.77 ± 0.48
Glx	7.34 ± 1.75	9.82 ± 5.17
Glutamate	2.75 ± 0.73	3.50 ± 2.62
Choline	1.98 ± 0.07	2.02 ± 1.65
Phosphocholine	2.74 ± 0.76	3.18 ± 2.01
Glycerophosphocholine	0.77 *	0.64 ± 0.30
Scyllo-Inositol	1.51 ± 0.74	1.00 ± 0.38
Taurine	1.43 *	1.63 ± 0.31
Myo-Inositol	1.48 *	1.94 ± 0.59
Glycine	0.47 *	1.43 ± 0.54
Glucose	0.10 *	0.36 ± 0.27

(*) Quantification performed on only one sample, since the other one presented contaminants in the analyzed spectral region.

Purpose of this experimental design was to analyze the metabolic changes occurring between tissue dissection and freezing for a better definition of correct procedures for preserve the native metabolic informations of tissues samples. In fact, degradation of labile metabolites is presently a major concern in HRMAS studies of tissues, since these reactions start at surgical dissection in the operative theater and continue during tissue handling before freezing at liquid nitrogen temperature, and also during MRS analysis **[25, 26]**.

The most relevant changes (p=0.04) occurred in the Cho signal with average 2-fold increases after 2h, 4-fold after 6h and 5-fold after 24h **(Fig. 14)**. PCho and GPC were practically unaltered until 6h and decreased by 50% at 24h. Parallel decreases were observed for taurine, while myo-inositol did not change appreciably.

Analysis of aqueous extracts confirmed an increase in Cho up to 26.5 ± 7.5 nmol/mg tissue at 24h.

Our results indicate that to preserve the metabolic integrity of the tissue and proceed to correct HRMAS analyses, the specimens should be frozen as quickly as possible after dissection and the elapsed time before freezing should be accurately recorded. Thus, the high Cho signals reported in several studies could be due to phospholipase-, phosphodiesterase- and phosphatase-mediated tissue

degradation occurring in the surgical theatre and then the relationships between MRS signals and clinical parameters should be taken into careful account **[26]**.

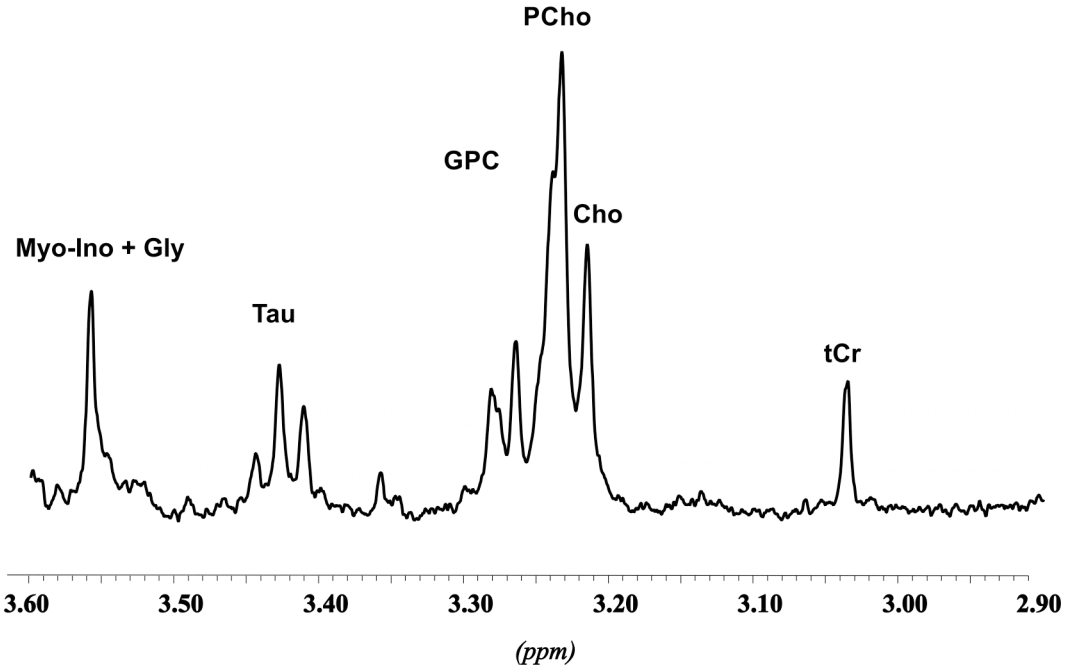

Figure 13. ^{1}H HRMAS spectrum of a surgical specimen isolated from a breast cancer patient.

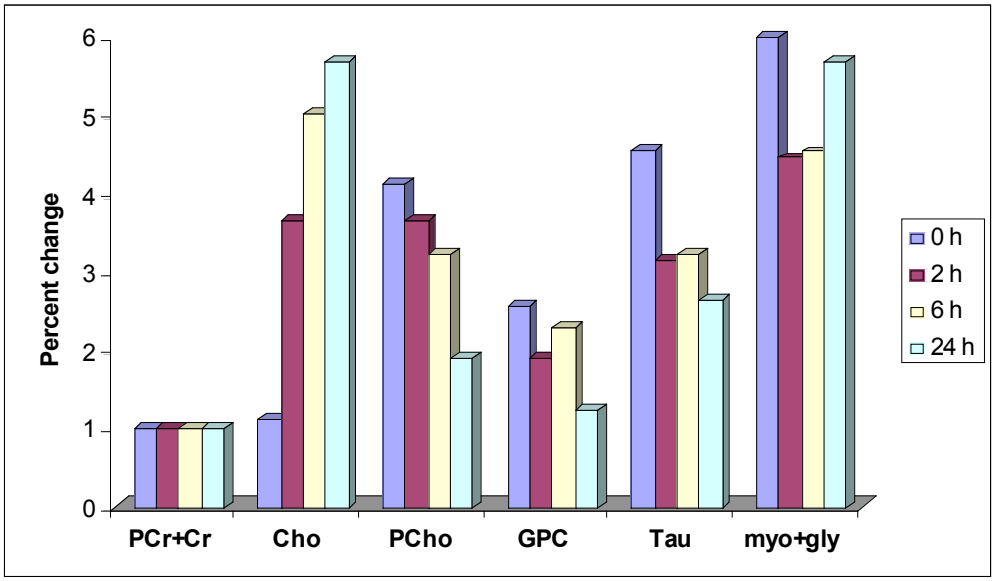

Figure 14. Percent change of relative metabolite levels (met/tCr) occurring in dissected breast tissue that was frozen at different times (10-40 min; 2, 6 and 24 h) after dissection.

Our studies by HRMAS analyses showed that the adopted of rigorous experimental procedures on all steps, beginning from tissue dissection until to MRS analysis, is essential for better understanding the molecular mechanisms underlying the detected spectral changes, especially in clinical samples. Since MRS can identify biochemical differences between cancer and non-tumoral tissues, this approach could improve the information provided by in vivo clinical ^{1}H MRS, because of the enhanced resolution of choline compounds in ex-vivo specimens.

CONCLUSION

^{1}H MRS studies conducted in preclinical ovary cancer provided acquisition of an integrated set of information on altered choline metabolism during tumor progression. Furthermore, we found that biosynthetic and catabolic PC-cycle enzymes contribute to the increased PCho levels.

With the aim of validating the clinical significance of tCho in surgical samples, we evaluated the changes in the levels of MRS-detected metabolites in ovary and breast tumour specimens at the time of surgery, and at different times before and during HRMAS analysis. We also performed analyses on tissue samples isolated from human EOC xenografts in immuno-deficient mice. The results suggested that the PCho content significantly decreased ($P=0.02$; $n=10$) in cisplatin-treated compared with untreated tumors, indicating that this metabolite may be considered as a possible endpoint of EOC therapy response.

The main results so far obtained were:

1. PCho and tCho levels increase in human EOC cell lines as compared to non tumoral EONT cells.
2. Two enzymes, ChoK and PC-plc, are responsible for PCho intracellular accumulation in EOC cells. These enzymes may be considered as molecular targets for anti-cancer treatment.
3. The inhibition of PC-plc with D609 was associated with about 50% drop in PCho content and slower proliferation rate with respect to untreated cells.
4. In EOC xenograft models, PCho, the most intense resonance in the tCho region, was not significantly altered by different in vivo and in vitro experimental growth conditions.
5. The observed PCho decrease in cisplatin-treated xenografts suggest that this signal could act as good indicator of in vivo response to therapy.
6. High choline content detected by ^{1}H HRMAS on human EOC clinical biopsies suggest that tissue degradation may occur even at relatively early phases of sample handling, storing and MRS analyses, pointing to the need of establishing rigorous procedures of tissue handling in the surgical theatre, in accordance with ad hoc Ethical Committee advice.

The body of evidences specifically acquired in this study on altered choline metabolism in ovary cancer cells and tissues warrants further efforts to elucidate the value of integrated current imaging modalities with the metabolic information provided by ^{1}H MRS approaches, to improve strategies for non invasive diagnosis and therapy response follow up.

ACKNOWLEDGMENTS

This work was continuously encouraged and sustained by Prof. Alfredo Colosimo, which I gratefully acknowledge.

APPENDIX

Epithelial ovarian non-tumoral and EOC cells

OSE cells were scraped from the surface of normal human ovaries obtained at surgery from patients affected by benign or malignant gynecological diseases other than ovarian carcinoma. All human materials were obtained with informed consent from patients. OSE cells were maintained in culture as previously described **[9]**. Stably immortalized non tumoral OSE cell variants, obtained by OSE transfection with the simian virus 40 (SV40) large T antigen (IOSE) and by further IOSE transfection with the cDNA of the catalytic subunit of the human telomerase reverse transcriptase (hTERT, kindly provided by Dr. R. A. Weinberg, Whitehead Institute, Cambridge, MA) were prepared and cultured as previously reported **[9]**. Details on the EOC cell lines utilized in the present study (IGROV1, OVCAR3, SKOV3 and CABA I) are also given in ref. **27**. All EOC lines were of ascitic origin, except IGROV1 which derived from a primary solid adenocarcinoma.

Tumor cell lines were maintained in RPMI-1640 (Gibco) supplemented with 10% (v/v) FCS and 2 mM L-glutamine (Sigma). All cells were cultured in a humidified atmosphere of 5% CO_2 at 37°C and routinely tested for mycoplasma infection using the mycoplasma PCR ELISA kit (Roche, Basel, Switzerland).

Epithelial ovarian cancer cells for xenograft models.

The following human serous ovarian carcinoma cell lines were used: **OVCA432** and **SKOV3** obtained from the American Type Culture Collection (ATCC), both of ascitic origin. The **SKOV3 ip** cell line was established from ascites developed in SCID mouse given an intraperitoneal (**i.p.**) injection of SKOV3 cells according to the protocol by Yu et al. **[28]**.

Animals.

4- to 6-week-old severe combined immunodeficiency (SCID) female mice were purchased from Charles-River. All animals were treated in accordance with protocols approved by the institutional authority in close agreement with European Community Directives and with the Italian Law. All efforts were made to minimize animal suffering and to reduce the number of animals used.

Subcutaneous xenograft models.

The cells in log phase (2 x 10^6) suspended in 0.2 ml of a solution containing a mixture (1:1) of growth medium and ice cold Matrigel (Beckton Dickinsons) were injected in the flank or in the back of SCID mice (5 to 7 weeks old). During growth, tumour weights (mg) were calculated, twice a week, by measuring with calipers the width and the length of each tumour in millimetres and by using the following formula: length x (width^2) *1/2 **[29]**.

Intraperitoneal xenograft models.

Ovarian cancer cells were suspended in growth medium at 8 x 10^6 cells/0.5mL and injected i.p. into 5- to 7- week-old SCID mice.

In vivo cisplatin treatments on tumour xenografts.

Fifteen days after the subcutaneous tumour cells implantation in SCID mice, we started the Cisplatin treatment [5mg/Kg], once a week for three weeks. At the end of the third week the animals were sacrificed, tumour tissues harvested and stored in liquid nitrogen until they were thawed and immediately analyzed with HR MRS.

Cell extracts in aqueous phase.

Cells grown to 60-70% confluence were trypsinized 24 h after culture medium change, counted, and assessed for viability (80-90%) and membrane integrity by Trypan blue staining. Cells were washed twice with ice-cold physiological saline solution and pellets resuspended in 0.5 mL of ice-cold twice-distilled water. Aqueous extracts (from 20-30 x 10^6 cells/sample) were prepared in EtOH:H_2O (70:30, v/v) according to an established protocol already described **[9].** Samples were ultra-sonicated at 20 kHz with an exponential probe, 8 μm peak-to-peak by a MSE ultrasonic disintegrator Mk2 (Crawley, Sussex, UK) and centrifuged at 14000 x g for 30 min. Supernatants were lyophylized twice in a RVT 4104 Savant lyophylizer (Mildford, Main, USA), and the residue resuspended in 0.7 ml D_2O (Sigma-Aldrich, Milan, Italy) containing 0.1 mM 3-(trimethylsilyl)-propionic-2,2,3,3-d4 acid sodium salt (TSP) as internal standard (Merck & Co, Montreal, Canada).

Immunohisto-chemistry.

Tumor tissues were fixed in 4% formaldehyde, paraffin-embedded, sectioned and processed for either hematoxylin-eosine (H&E) staining or immunohistochemical staining. For immunohistochemistry, sections were incubated with primary antibodies, followed by peroxidase-conjugated secondary antibodies.

APPENDIX2

List of the principal abbreviations:

MRS	magnetic resonance spectroscopy
HRMAS	high resolution magic angle spinning
tCho	choline containing compounds
PCho	phosphocholine
GPC	glycerophosphocholine
Cho	free choline
EONT	epithelial ovarian non tumoral
OSE	ovarian surface epithelial
IOSE	immortalized ovarian surface epithelial
hTERT	human telomerase reverse transcriptase
EOC	epithelial ovarian cancer
PC	phosphatidylcholine
Chok	choline kinase
PC-plc	phosphatidilcholine specific phospholipase C
pld	phospholipase D
GPC-pd	glycerophosphocholine phosphodiesterase

REFERENCES

1. Negendank WG. Studies of human tumors by MRS: a review. NMR Biomed 1992; 5: 303-24.

2. Podo F. Tumour phospholipid metabolism. Review article. NMR Biomed 1999; 12: 413-39.

3. Gillies RJ, Morse DL. In vivo magnetic resonance spectroscopy in cancer. Annu Rev Biomed Eng 2005; 7: 287-326.

4. Glunde K, Ackerstaff E, Mori N, Jacobs MA, Bhujwalla ZM. Choline phospholipid metabolism in cancer: consequences for molecular pharmaceutical interventions. Mol Pharm 2006; 3: 496-506.

5. Aboagye EO, Bhujwalla ZM. Malignant transformation alters membrane choline phospholipid metabolism of human mammary epithelial cells. Cancer Res 1999; 59: 80-4.

6. Glunde K, Jie C, Bhujwalla M. Molecular causes of the aberrant choline phospholipid metabolism in breast cancer. Cancer Res 2004; 64:4270-76.

7. Eliyahu G, Kreizman T, Degani H. Phosphocholine as a biomarker of breast cancer: molecular and biochemical studies. Int J Cancer 2007;120:1721-30.

8. Jemal A, Siegel R, Ward E, Hao Y, Xu J, Murray T, Thun MJ. Cancer statistics, 2008. CA Cancer J Clin. 2008;58:71-96.

9. Iorio E, Mezzanzanica D, Alberti P, Spadaro F, Ramoni C, D'Ascenzo S, Millimaggi D, Pavan A, Dolo V, Canevari S, Podo F. Alterations of choline phospholipid metabolism in ovarian tumor progression. Cancer Res 2005; 65: 9369-76.

10. Iorio E, Ricci A, Pisanu ME, Paris L, Di Vito M, Castellano G, Bagnoli M, de Cecco L, Glunde K, Bhujwalla Z, Mezzanzanica D, Canevari S and Podo F. Genomic and molecular characterization of enzymes contributing to phosphocholine MRS signal in ovary cancer. ISMRM 2009. Abstract N°2312.

11. Ricci A, Iorio E, Podo F. Alterations of Choline Phospholipid Metabolism in Ovarian Timour Progression: a NMR Study. Biophysics and Bioengineering Letters 2008; 1:1-8. http://padis2.uniroma1.it:81/ojs/index.php/CISB-BBL.

12. Podo F, Carpinelli G, Ferretti A, Borghi P, Proietti E, Belardelli F. Activation of glycerophosphocholine phosphodiesterase in Friend leukemia cells upon in vitro-induced erytroid differentiation.31P and 1H NMR studies. *Israel J.Chem* 1992;32:47-54.

13. Ramirez de Molina A, Gutierrez R, et al. Increased choline kinase activity in human breast carcinomas: clinical evidence for a potential novel antitumor strategy. Oncogene 2002; 21: 4317-22.

14. Ramírez de Molina A, Sarmentero-Estrada J, Belda-Iniesta C, Tarón M, Ramírez de Molina V, Cejas P, Skrzypski M, Gallego-Ortega D, de Castro J, Casado E, García-Cabezas MA, Sánchez JJ, Nistal M, Rosell R, González-Barón M, Lacal JC. Expression of choline kinase alpha to predict outcome in patients with early-stage non-small-cell lung cancer: a retrospective study. Lancet Oncol 2007;8:889-97.

15. Glunde K, Raman V, Mori N, Bhujwalla ZM. RNA interference-mediated choline kinase suppression in breast cancer cells induces differentiation and reduces proliferation. Cancer Res 2005; 65: 11034-43.

16. Al-Saffar NM, Troy H, Ramirez de Molina A, et al. Non invasive magnetic resonance spectroscopic pharmacodynamic markers of the choline kinase inhibitor MN58b in human carcinoma models. Cancer Res 2006; 66: 427-34.

17. Ramoni C, Spadaro F, Barletta B, Dupuis ML, Podo F. Phosphatidylcholine-specific phospholipase C in mitogen-stimulated fibroblasts. Exp Cell Res. 2004, 299:370-82.

18. Spadaro F, Ramoni C, Mezzanzanica D, Miotti S, Alberti P, Cecchetti S, Iorio E, Dolo V, Canevari S, Podo F. Phosphatidylcholine-specific phospholipase C activation in epithelial ovarian cancer cells. Cancer Res. 2008; 68:6541-9.

19. Ricci A, Cecchetti S, Iorio E, Pisanu M, Paris L, Portella L, Scala S, Podo F. Relationship between CXCR4/CXCL12 axis and phosphatidylcholine cycle in a human lymphoblastoid cell line monitored by ^{1}H MRS. ESMRMB 2009. Abstract accepted.

20. Canese R, Iorio E, Ricci A, Pisanu ME, Giannini M, Podo F. Metabolites quantification in tumours by magnetic resonance spectroscopy: objectives, results and perspectives. CMIR. 2009; 5:110-27.

21. Cheng LL, Chang IW, Louis DN, Gonzalez RG. Correlation of high-resolution magic angle spinning proton magnetic resonance spectroscopy with

histopathology of intact human brain tumor specimens. Cancer Res. 1998, 58:1825-32.

22. Sitter B, Lundgren S, Bathen TF, Halgunset J, Fjosne HE, Gribbestad IS. Comparison of HR MAS MR spectroscopic profiles of breast cancer tissue with clinical parameters. NMR Biomed. 2006; 19:30-40.

23. van Asten JJ, Cuijpers V, Hulsbergen-van de Kaa C, Soede-Huijbregts C, Witjes JA, Verhofstad A, Heerschap A. High resolution magic angle spinning NMR spectroscopy for metabolic assessment of cancer presence and Gleason score in human prostate needle biopsies. MAGMA. 2008;21:435-42.

24. Cheng LL, Ma MJ, Becerra L, Ptak T, Tracey I, Lackner A, González RG. Quantitative neuropathology by high resolution magic angle spinning proton magnetic resonance spectroscopy. Proc Natl Acad Sci U S A. 1997;94:6408-13.

25. Swanson MG, Zektzer AS, Tabatabai ZL, Simko J, Jarso S, Keshari KR, Schmitt L, Carroll PR, Shinohara K, Vigneron DB, Kurhanewicz J. Quantitative analysis of prostate metabolites using 1H HR-MAS spectroscopy. Magn Reson Med. 2006;55:1257-64.

26. Ricci A, Iorio E, Pisanu M, Cappelletti V, Mezzanzanica D, Canevari S, Podo F. Alterations of ^{1}H MRS HR-MAS signals of human breast carcinoma following dissection of surgical specimens. ESMRMB 2009. Abstract accepted.

27. Ferretti A, D'Ascenzo S, Knijn A, Iorio E., Dolo V, Podo F. Detection of polyol accumulation in a new ovarian carcinoma cell line, CABA 1: a 1H NMR study. Br J Cancer 2002; 86: 1180-87.

28. Yu D, Wolf JK, Scanlon M, Price JE, Hung MC. Enhanced c-erbB-2/neu expression in human ovarian cancer cells correlates with more severe malignancy that can be suppressed by E1A. Cancer Res. 1993; 53:891-8.

29. Han LY, Landen CN, Trevino JG, Halder J, Lin YG, Kamat AA, Kim TJ, Merritt WM, Coleman RL, Gershenson DM, Shakespeare WC, Wang Y, Sundaramoorth R, Metcalf CA 3rd, Dalgarno DC, Sawyer TK, Gallick GE, Sood AK. Antiangiogenic and antitumor effects of SRC inhibition in ovarian carcinoma. Cancer Res 2006; 66:8633-9.